SERI/STR-211-2760
(DE85016847)

Energy SOLAR

DIAGNOSTICS OF GLOW DISCHARGES USED TO PRODUCE HYDROGENATED AMORPHOUS SILICON FILMS

A Subcontract Report for the Period April 15, 1984—April 14, 1985

By
A. Gallagher
J. Scott

July 1985

Work Performed Under Contract No. AC02-83CH10093

National Bureau of Standards
Boulder, Colorado

and

Solar Energy Research Institute
Golden, Colorado

Technical Information Center
Office of Scientific and Technical Information
United States Department of Energy

DISCLAIMER

Available from the National Technical Information Service, U. S. Department of Commerce, Springfield, Virginia 22161.

Price: Printed Copy A03
Microfiche A01

Codes are used for pricing all publications. The code is determined by the number of pages in the publication. Information pertaining to the pricing codes can be found in the current issues of the following publications, which are generally available in most libraries: *Energy Research Abstracts (ERA); Government Reports Announcements* and Index *(GRA* and I); *Scientific and Technical Abstract Reports (STAR);* and publication NTIS-PR-360 available from NTIS at the above address.

Printed in the United States of America
USDOE Office of Scientific and Technical Information
Oak Ridge, Tennessee

SERI/STR-211-2760
(DE85016847)
Distribution Category UC-63

Diagnostics of Glow Discharges Used to Produce Hydrogenated Amorphous Silicon Films

A Subcontract Report
15 April 1984 - 14 April 1985

A. Gallagher (National Bureau of Standards) **and**
J. Scott (University of Colorado — Boulder),
Principal Investigators

National Bureau of Standards
Boulder, Colorado

Prepared under Subcontract No. DB-4-04078-1

SERI Technical Monitor: Werner Luft

Solar Energy Research Institute
A Division of Midwest Research Institute

1617 Cole Boulevard
Golden, Colorado 80401

Prepared for the
U.S. Department of Energy
Contract No. DE-AC02-83CH10093

TABLE OF CONTENTS

FIGURES

TABLE

ABSTRACT

Measurements of monosilane and disilane radicals have been made at the surface of dc glow discharges (GD) in pure silane and silane-argon mixtures. These observations have been interpreted in terms of discharge kinetic models, and from this we have inferred that the dominant radical, SiH_3, is produced in the gas and is primarily responsible for film growth. We conclude that the heavier radicals observed in the gas are primarily a consequence of surface reactions, as is the disilane which is a major product of the monosilane decomposition. In addition, we have carried out a detailed model of the ion chemistry in the discharge, deriving theoretical distributions of ions at the cathodes of low-pressure dc discharges.

Chemical vapor deposition rates of silane and disilane, which have been measured previously in our laboratory, have now also been interpreted in detail to yield a self-consistant model for the CVD process. This model identifies and quantifies the role of H_2 as an inhibitor of silane GD and CVD deposition. Implications of these discoveries to deposition rates and film properties are discussed.

SUMMARY

The purpose of this work is to improve the understanding of (a) the processes leading to a-Si:H film growth in silane glow discharges (GD), and (b) the film characteristics. This is done by observing the gas species responsible for the gas chemistry and film growth, particularly the neutral radicals.

We have previously reported observation of the nonsilane radicals SiH_n(n=0-3), and the dominance of SiH_3 within these [1]. A primary goal for this contract year was to increase our sensitivity and discrimination for radial detection, to allow accurate measurement of the minor constituents Si, SiH, and SiH_2, as well as of the disilane radicals Si_2H_n(n=0-3). This was achieved; the results have been reported at the contractors annual revue meeting [2] and are being prepared for publication. Measurements under a variety of discharge conditions and for dc and rf discharges are now needed.

A second goal for this contract year (April 1984-April 1985) was to utilize this increased radical sensitivity to measure film properties vs. different mixtures of depositing radicals. This goal was a logical consequence of the assumption that the radicals were formed in the glow discharge and then deposited on the substrate. Thus, learning to control the gas radical mixture should allow control of the depositing species and thereby the film properties.

Midway through the year, we compared our newly-measured, complete set of radical densities with our discharge chemistry models, and realized that many of the radicals were actually being released from surfaces. This must result from surface reactions and sputtering. Thus the assumed sequence of radical production in the gas, followed by deposition is incorrect, as is the assumption that the gas might be independently prepared in mixtures that determine film properties. Instead, the radicals in the gas depend on the film surface properties. Thus, until the surface processes are better understood the value of our original goal is unclear; we have therefore postponed it. However, this discovery provides an opportunity to study the film growth itself, as the Si_xH_n molecules released from the surface depend on the species and reactions leading to silicon incorportation and film morphology. We have therefore shifted the emphasis of the original goal toward developing an understanding of the film-growth process, and how this can be controlled to optimize film quality.

The thermal decomposition (CVD) of silane on hot a-Si:H surfaces involves many of the same surface reactions that occur in GD deposition, but for unknown reasons CVD produced photovoltaics are not yet as good as those made by glow discharges. To investigate this question and the processes involved in film growth we have measured the decomposition of

silane and hot a-Si:H surfaces. From analysis of a wide range of data we have now developed a surface-reaction model that explains the basic steps involved in GD depositions of SiH_3 and in CVD deposition of SiH_4. The University of Colorado Ph.D. thesis of R. Robertson, containing these models and data, has been completed, and a publication is in preparation. This model is an initial step towards understanding the causes of different bulk-film characteristics (e.g. the number of SiH_2 vs. SiH sites), and we have additional studies planned and under way to delineate additional details in the CVD and GD film-growth processes.

We have completed a calculation of the ion chemistry and species in dc silane discharges, with emphasis on those arriving at the cathode. This calculation is an essential step in understanding cathodic films, the sputtering release of radicals from the surface, and discharge diagnostics. This calculation required analysis of ion production and reactions in the varying elastic field of the discharge sheath. Additional measurements of the ion energy distributions at the substrate are planned, as this is important to film damage, growth and sputtering.

SECTION 1.0

INTRODUCTION

During the past year we have continued to use mass spectrometry of the neutral species produced in silane discharges, for discharge parameters and conditions that match those typically used by various laboratories to obtain good photovoltaic devices. We have continued to study primarily low-pressure, low power dc discharges rather than rf, since these are more readily controllable and have been used by RCA and Solarex to produce some of the highest efficiency cells. Based on our models and on survey-type measurements, we believe that many of our observations in dc discharges also apply, with minor modifications, to rf discharges.

Due to the complexity of the many processes that can occur in these discharges, it is important to utilize detailed diagnostics. Consequently, we have developed methods to measure the radical species in these discharges. These species are present in very low densities, but they are responsible for the neutral chemistry in the discharge and the film growth. We have increased our sensitivity for detecting these neutral radical species, as well as our ability to discriminate against background gas and other interfering signals. In addition, we have extended our measurements from those of the monosilane radicals, SiH_n, to the disilane radicals, Si_2H_n. We now have a sensitivity of better than one part per million of the total gas pressure, and we can detect radical densities on the order of 10^8 cm^{-3}.

We found some very major surprises from the radical measurements. In particular, measuring radicals at the cathode of a dc discharge, we observed that very high densities of disilane radicals (larger than the SiH_3 density in some cases) were present. These densities exceeded anything we could explain on the basis of gas reactions of the monosilane radicals produced in the discharge, or electron collisions with disilane produced by the discharge. More detailed measurements are needed to totally separate the roles of gas and surface processes, but it has nonetheless become clear that we are observing primarily heavy radicals released from surfaces of the discharge. (Sputtering from the cathode is probably the major cause of the release of these radicals in dc discharges. Sputtering from both electrodes occurs in rf discharges.) This surface release of radicals complicates the problem of characterizing or preparing the gas mixture whose depositing species are responsible for the film characteristics. On the other hand, it allows us the opportunity to observe consequences of the film-growth reaction processes, since products of these surface reactions are being released into the gas and observed by our mass spectrometry. With this opportunity in mind, we are now developing more detailed models of the surface, its morphology, and its interaction with the radical and stable neutral gases in the discharge.

It is well known that films made at the cathode of dc discharges have poor photovoltaic properties; this has been attributed to imperfections produced by energetic ion impact on the film [3,4]. The use of a cathode screen in front of the gounded substrate (a "dc-proximity" discharge) eliminates essentially all of the ion bombardment of the substrate and yields much better film quality. Substrate ion bombardment also occurs in rf discharges, although the ion currents and energies are considerably lower than at dc discharge cathodes. Nonetheless, many laboratories have grown good photovoltaics on the electrodes of rf discharges. A screen above the substrate, electrically connected to the substrate base, also eliminates most of this substrate ion bombardment in rf discharges, but the reported effect of this on film quality is not yet clear cut. Film bombardment by low energy ions could be valuable, for example by removing dangling macro-molecules and by assisting rearrangement of highly distorted Si-Si bonds. We think that introducing such a screen and varying its rf impedance and/or bias to the substrate base would be an easy method of controlling the substrate ion bombardment, and perhaps improving film quality thereby.

In addition to these direct effects of bombardment of films, our observations point to the presence of many radicals in the gas due to electrode bombardment and surface reactions. This will occur in screened or unscreened dc or rf discharges. If the substrate is protected by a screen, these radicals will come primarily from the screen and many will deposit on the substrate, often after modification by gas reactions. If no screen is used, they will be released from the substrate and redeposited on it, but often in different form due to gas reactions. As a first step in exploring this complicated interplay we have so far concentrated on determining which species are released from a dc-discharge cathode. We find that these species constitute a significant fraction of all radicals in the gas; thus they make an important contribution to the film growth and must be considered in detail.

During the latter part of this year we have put a major effort into diagnosing our current and previous data to delineate the reactions that occur on the growing amorphous silicon surface. In particular, we have attempted to develop a surface model that encompasses CVD as well as glow-discharge deposition data. This model is still very preliminary, but it includes surface reactions of the silane, disilane, and H_2 as well as of the radical species. We are now initiating experiments which will separate and more accurately delineate these surface processes, which are crucial in determining the film structure.

In addition to these studies of the neutral species in the discharge, we are continuing our analyses of the ion species in order to verify our understanding of the electron collision and ion collision processes taking place in the discharge. In addition, the distribution

of species and ion energies of the ions impinging on the substrate surface are believed to be important in understanding the surface growth and the release of surface molecules back into the gas. We report here the results of a detailed modeling of the electron collision processes producing the ions, and of the ion-molecule reactions that take place as ions drift to the cathode of a dc discharge. This gives us the capability of making quantitative comparisons between theory and measurements of the ions impinging on the cathode. This work is reported by Chatham and Gallagher in a paper that will appear in the Journal of Applied Physics (Ref. 9.).

A detailed description of our silane discharge radical measurements is in the University of Colorado Ph.D. thesis of R. Robertson (unpublished). This was completed in May, 1985. A summary of the essential features of these measurements and models is included here, in the following sections.

Under the direction of J. Scott, Raman spectra of a-Si:H and a-Si:Sn:H films have been made using films made at SERI. A summary of these observations is given below, in Sec. 6.0.

SECTION 2.0

DISCHARGE MEASUREMENTS

As described previously [1], we utilize an electron-beam ionizer and mass spectrometer to detect stable and radical gas species emanating from a small sampling hole in the discharge. The stable molecules Si_xH_{2x+2} are easily identified by their ion masses. The radicals SiH_n ($n = 0-3$) are separated from the much larger density SiH_4 by utilizing threshold ionization and the typically 4 eV lower threshold for $e + SiH_n \rightarrow SiH_n^+$ compared to $e + SiH_4 \rightarrow SiH_n^+ +$ products. Si_2H_n radicals ($n = 0-5$) are similarly separated from signals at the same mass due to dissociative ionization of Si_2H_6.

The most universal index of discharge power and flow is the fraction f of silane decomposed while flowing through the discharge. The change ΔN in silane density N, when turning the discharge on, yields a direct measure of $f = \Delta N/N$. We have observed that $f \propto P/F$ for a wide range of discharge power P and flow F, as is expected since the discharge energy deposited, per silane molecule, is proportional to P/F. Essentially all laboratories report that films with optimum photovoltaic properties are obtained at high flows and low powers, and from our observations the quoted optimum P and F values correspond to $f < 0.1$. Thus, we have studied small-f discharge conditions, subject to the constraint that radical signal sizes are also proportional to f.

In order to observe the initially produced radical species, before radical-silane reactions occur, it is necessary to operate at very low SiH_4 densities, where few radical-SiH_4 collisions occur before the radicals reach the surface. In order to operate a discharge at these low SiH_4 densities, we have studied discharges in Ar/SiH_4 mixtures. In Fig. 2.1 the density of disilane $[Si_2H_6]$ formed by the discharge is compared to ΔN in a dc discharge in a 5 mT (millitorr) silane-45 mT argon mixture with a room temperature substrate. The ratio $2[Si_2H_6]/\Delta N$, shown in Fig. 2.1, is the fraction of the Si from decomposed SiH_4 that is processed into (and pumped away as) Si_2H_6. As the discharge current i approaches zero, this ratio approaches 30%, but as the power increases this disilane is decomposed in the discharge and the ratio decreases.

At the low density chosen for this experiment, SiH_n radicals produced in the discharge diffuse rapidly to the surface, so that radical densities are small and radical-radical reactions do not occur in the gas. Of the SiH_n radicals formed in electron collisional dissociation of silane, only SiH_2 can react with SiH_4 to form Si_2H_6. The rate for this reaction is very slow at these low pressures, and in addition we expect SiH_2 to be a minor constituent of the dissociation products [1]. Thus, the observed Si_2H_6 cannot be attributed to this reaction. Si is also a very minor initial dissociation product, and can only form Si_2H_6 by multiple

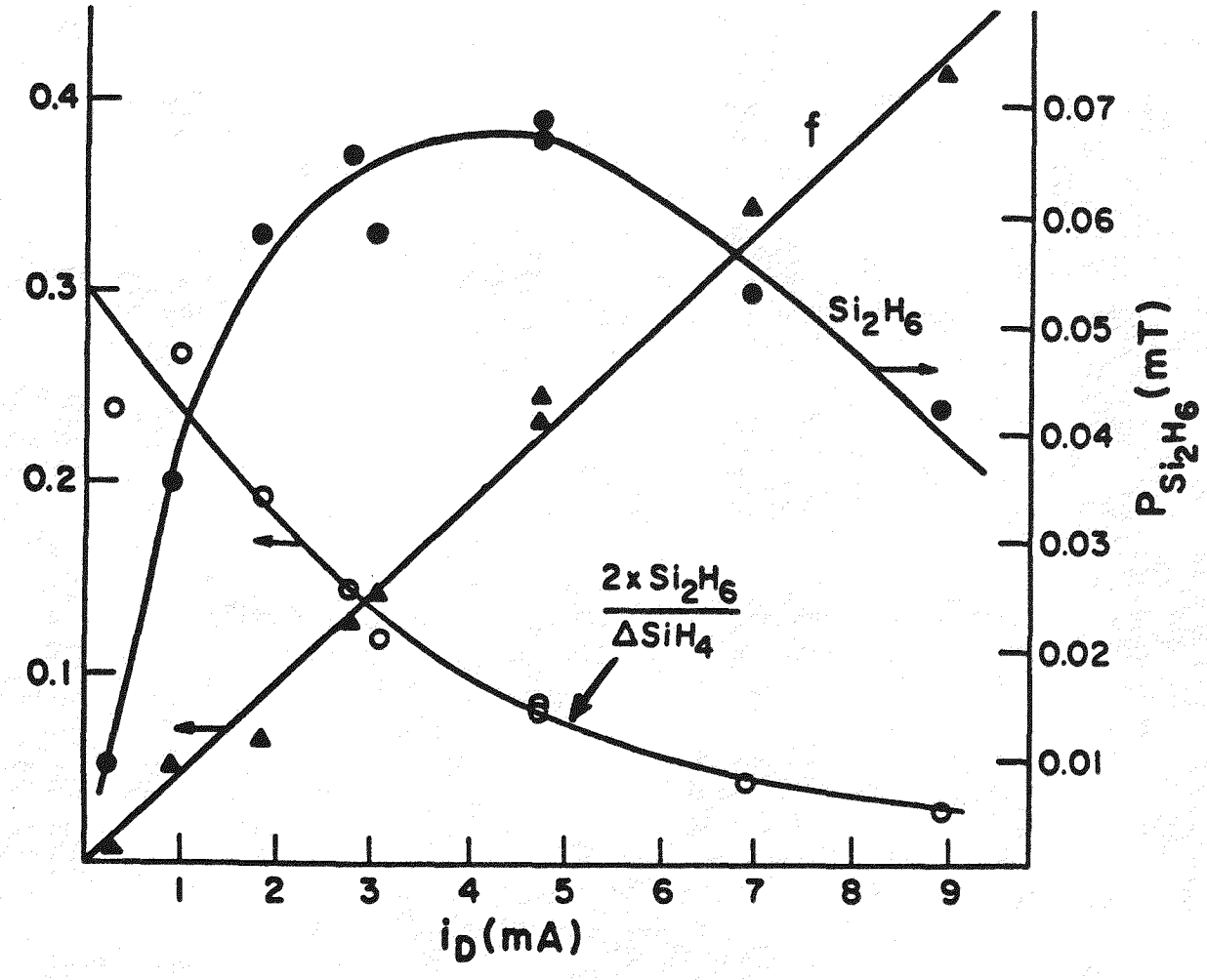

Fig. 2.1. Silane depletion fraction (f, left scale), Si_2H_6 pressure (right scale), and fraction of Si atoms from depleted silane that are incorporated into Si_2H_6, for a dc discharge in 5 mTorr SiH_4 and 45 mTorr Ar.

reactions. SiH and SiH_3 do not form Si_2H_6 in gas reactions. One concludes that almost all Si_2H_6 is formed by surface reactions and released into the gas. Consistent with this, Longeway et al. [5] have recently inferred that a great detail of Si_2H_6 is formed on the a-Si:H surface.

As we have previously reported [6], ~60% of the Si from decomposed silane is pumped away as Si_2H_6 in low-power pure silane discharges, with the remainder primarily incorporated into film. It is not yet determined if this increase from 30% to 60% is due to gas or surface reactions.

The SiH_n (n = 0-3) radical densities at the cathode surface of a dc discharge in silane-argon mixtures have been measured as a function of discharge power and silane/argon ratio. We observe that SiH_3 is the dominant SiH_n specie under all conditions. Within experimental uncertainties of about a factor of 2 we have also observed that for fixed gas flow the ratio $[SiH_3]/\Delta N$ is independent of gas mixture and power. The ratios of other radical densities $[SiH_n]/[SiH_3]$, as a function of gas mixture, are shown in Fig. 2.2.

Our interpretation of these data is that about 90% of the SiH_4 dissociations by electron impact leave the Si atom in an SiH_n^+ ion or in SiH_3. In pure silane the ensuing fast $SiH_2^+ + SiH_4 \rightarrow SiH_3^+ + SiH_3$ reaction makes still more SiH_3, and many H atoms released in the initial silane decompositions undergo $H + SiH_4 \rightarrow SiH_3 + H_2$ reactions to make still more SiH_3. Overall, we conclude that in pure silane more than 90% of the SiH_n radicals produced in the gas should be SiH_3. This is consistent with the right side (pure silane) of Fig. 2.2. The increase in Si, SiH, and SiH_2 at the left side of Fig. 2.2 (primarily Ar) is partly due to loss of SiH_2^+ and H at the wall before reacting to form SiH_3. It might also be partly attributed to $Ar^+ + SiH_4$ or $Ar^m + SiH_4$ (metastable Ar) collisions, but our previous drift-tube experiments [7] rule out the former and present knowledge of $e + Ar \rightarrow Ar^m$ and Ar^m + molecule dissociation cross sections make the latter unlikely [8]. Overall, it appears just possible to explain the SiH_2 at the left side of Fig. 2.1, but not the large amounts of Si and SiH. Thus, these data suggest that most of the observed Si and SiH and possibly also SiH_2 are being released from the surface, probably due to ion-bombardment sputtering.

No reactions of SiH_3 with SiH_4 are exothermic, while $SiH_3 + SiH_4 \rightarrow Si_2H_5 + H_2$ has $\Delta H \sim 0$ (see Table 2.1). Thus, we attribute the nearly constant ratio $[SiH_3]/\Delta N$ in pure silane to the fact that about 2/3 of the Si atoms from decomposed SiH_4 become SiH_3 (the rest are SiH_n^+), and this SiH_3 reacts slowly with SiH_4, thereby reaching the surface as SiH_3. In a pure-silane, deposition discharge a major fraction of the Si, SiH, and SiH_2 initially produced by electron collision reacts with SiH_4 before reaching a surface. Thus, almost all surface deposition is due to SiH_3, with a small fraction from heavier radical products of gas reactions.

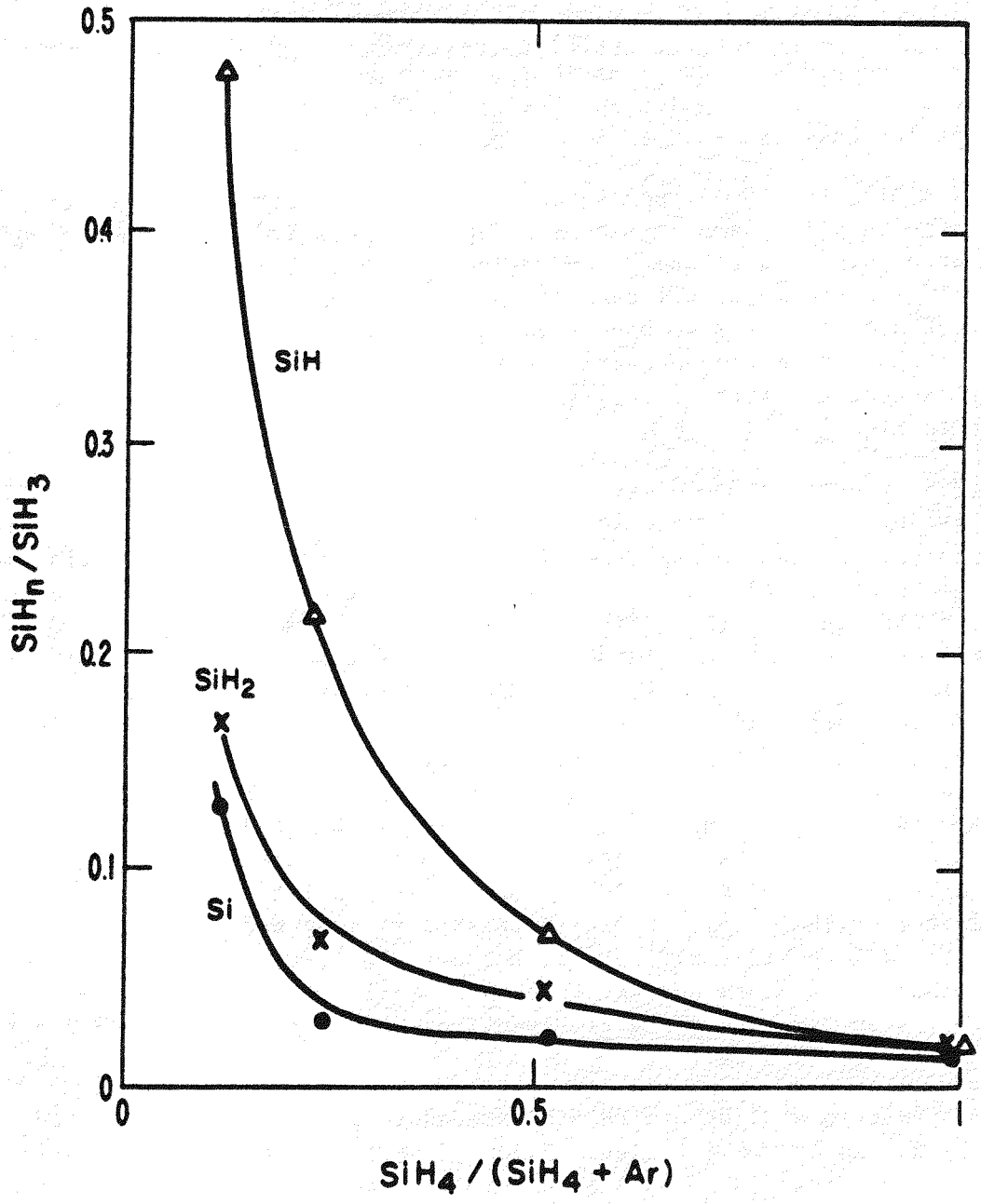

Fig. 2.2. Ratio of the SiH_n to the dominant SiH_3 radical, for n = 0-2, at the cathode of a dc discharge in 80 mTorr of gas silane. The abscissa is the fraction of silane in the silane/Ar mixture. The discharge power and flow were adjusted to produce ~10% silane depletion.

Table 2.1. Gas and surface reaction of monosilicon radicals. Reaction enthalpies are given in kcal/mole; those shown in parentheses are estimated. The reactions are numbered in the right column.

$Si + SiH_4 \rightarrow Si_2H_4^*$	-51.4	1
$\rightarrow 2SiH_2$	+1.3	2
$\rightarrow Si_2H_2 + H_2$	-12.9	3
$SiH_2 + SiH_4 \leftrightarrow Si_2H_6^*$	-47.7	4
$Si_2H_6^* + M \rightarrow Si_2H_6$	---	5
$Si_2H_6^* \rightarrow Si_2H_4 + H_2$	-2.3	6
$\rightarrow Si_2H_2 + 2H_2$	+36.2	7
$H + SiH_4 \rightarrow SiH_3 + H_2$	-13.9	8
$\rightarrow SiH + 2H2$	+22.7	9
$SiH + SiH_4 \rightarrow Si_2H_5^*$	-37.9	10
$\rightarrow Si_2H_3 + H_2$	-7.2	11
$SiH_3 + SiH_4 \rightarrow SiH_4 + SiH_3$	0	12
$\rightarrow Si_2H_6 + H$	+16.6	13
$\rightarrow Si_2H_5 + H_2$	-1.3	14
$Si_2H_5 + SiH_4 \rightarrow Si_3H_7 + H_2$	---	15
$\rightarrow Si_2H_6 + SiH_3$	+4.0	16

Table 2.1. (continued)

$Si_3H_7 + SiH_4 \rightarrow Si_4H_9 + H_2$	---	17
$\rightarrow Si_3H_8 + SiH_3$	---	18
$SiH_3 + SiH_3 \rightarrow Si_2H_6^{**}$	-73.7	19
$\rightarrow SiH_2 + SiH_4$	-26.0	20
$Si_2H_6^{**} \rightarrow SiH_2 + SiH_4$	-26.0	21
$\rightarrow Si_2H_4 + H_2$	-29.1	22
$\rightarrow Si_2H_2 + 2H_2$	+9.4	23
$Si_2H_6^{**} + M \rightarrow Si_2H_6$	---	24
$SiH_3 + H_{wall} \rightarrow SiH_{3\ ads} + H_{wall}$	(-12)	25
$H_{wall} + SiH_{3\ ads} \rightarrow SiH_{4\ ads} + b$	(0)	26
$SiH_{4\ ads} + b \rightarrow SiH_4 + b$	(+12)	27
$\rightarrow SiH_{3\ wall} + H$	(+15)	28
$\rightarrow SiH_{2\ wall} + H_2$	(0)	29
$SiH_{3\ ads} + b \rightarrow SiH_{3\ wall}$	(-90)	30
$SiH_{3\ ads} + SiH_{3\ ads} \rightarrow Si_2H_{6\ ads}^{**}$	(-80)	31
$b + b \rightarrow$ Si-Si bond	(-90)	32

The same threshold-ionization technique has been used to measure the Si_2H_n (n = 0-5) radicals produced in the discharge (see Fig. 2.3). However, in this case the $e + Si_2H_n \rightarrow Si_2H_n^+$ signals must be separated from a $e + Si_2H_6 \rightarrow Si_2H_n^+$ background due to Si_2H_6 made in the discharge. Turning the discharge off removes the background Si_2H_6 as well as the radicals, so we have instead used a beam-alignment method to separate these signals. Moving the discharge aperture out of alignment with the mass-spectrometer-ionizer apertures eliminates the radicals signals, as the radicals do not survive many surface collisions. The Si_2H_6 still reaches the mass spectrometer ionizer as background gas. These "in" and "out-of" alignment signals are shown at the right side of Fig. 2.4 for the $Si_2H_3^+$ ion. The difference is due to a (constant) leakage of $Si_2H_3^+$ ions from the discharge, plus the $e + Si_2H_3 \rightarrow Si_2H_3^+$ signal, with a threshold at ~8 eV. The signals obtained in this manner for all of the Si_2H_n radicals (after subtraction of the discharge-ion background) are shown on the left side of Fig. 2.4. The slope of each of these signals and the SiH_3^+ signal in the region 1 eV above threshold yields, with a minor adjustment for expected relative cross sections, these radical densities relative to SiH_3. This ratio, for each mass, is shown in Fig. 2.5 for discharges in pure silane and in a silane-argon mixture. Each mass M can be identified primarily with Si_2H_n, with n = M-56, as indicated in Fig. 2.5. A correction of ~10% due to heavier isotopes is necessary for M > 56, and the "radical" signal seen at M = 62 is attributed to such heavier isotopes.

The most impressive and surprising characteristic of the data in Fig. 2.5 is that the total Si_2H_n radical density exceeds the SiH_3, or total SiH_n, density for the silane-argon mixture. This measurement was made with very low silane density, such that a major fraction of the SiH_n radicals reach the surface before reacting with SiH_4. The most abundant SiH_n radical, SiH_3, can form Si_2H_5 in a gas reaction, possibly explaining some of the observed Si_2H_5 (M = 61). However, the observed densities of the other Si_2H_n radicals in the silane-argon case exceed those attributable to gas reactions by about a factor of 10 (see Sec. 3.0). Electron collisional dissociation of Si_2H_6 is another possible source of these heavier radicals. If Si_2H_2 and Si_2H_4 had a very small wall reaction rate, compared to SiH_3, this might explain their large densities. However, sputtering from the growing a-Si:H surface is a much more likely explanation. As discussed further below, surface reactions can also cause release of Si_2H_6 and of Si_2H_n radicals. We are initiating experiments designed to separate these different sources of the observed radicals.

The radical densities observed in Fig. 2.5 from the pure silane discharge can be partly a result of gas collisions, partly due to electron collisional dissociation of Si_2H_6, and partly from surface release of the radicals. Only highly endothermic gas reactions can produce the observed Si_2 and Si_2H, so these are not a result of gas reactions. Measurements as a function of $[Si_2H_6]/[SiH_4]$, time, and gas mixtures are planned to isolate the sources of these radicals.

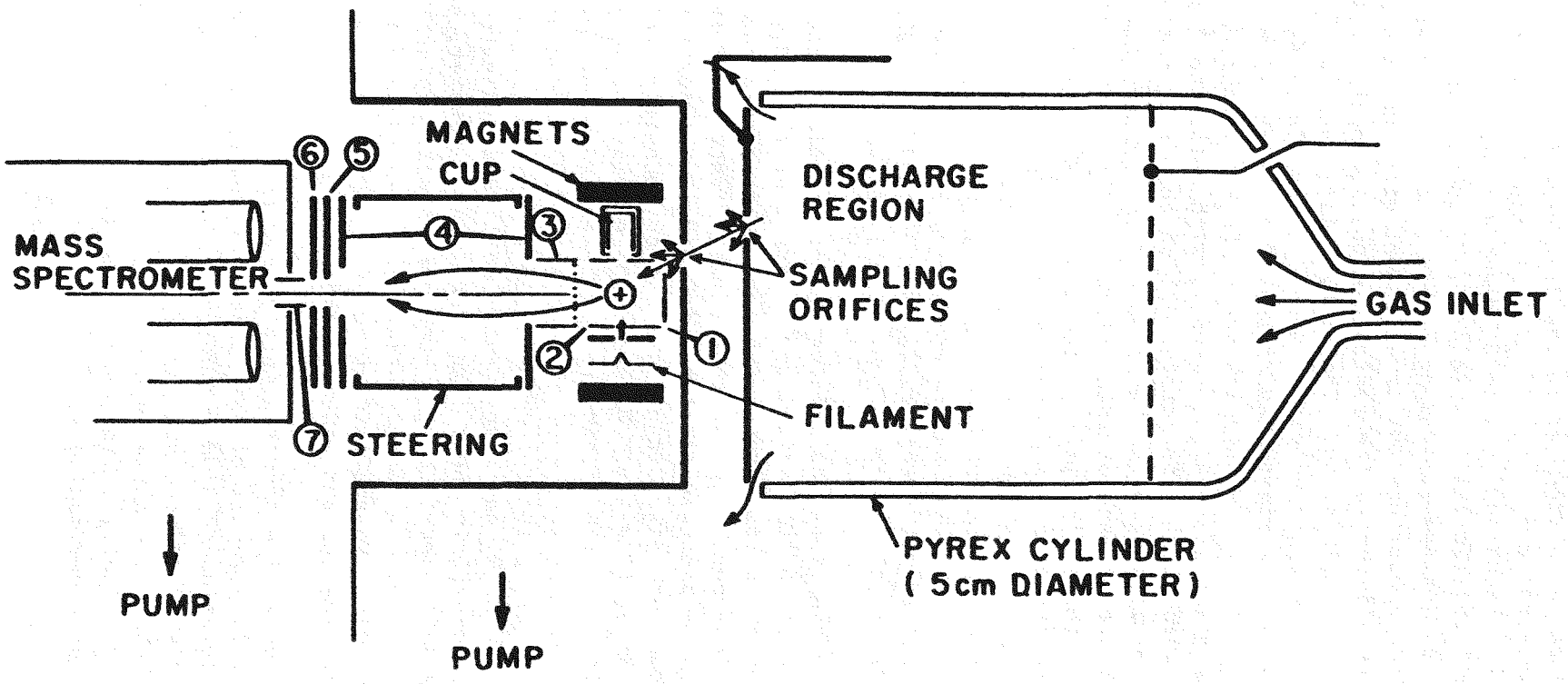

Fig. 2.3. Apparatus used to measure neutral and radical species at the substrate of silane discharges, approximately to scale. The discharge region is shown as set up for rf and dc discharges; an additional screen is introduced for dc proximity discharges.

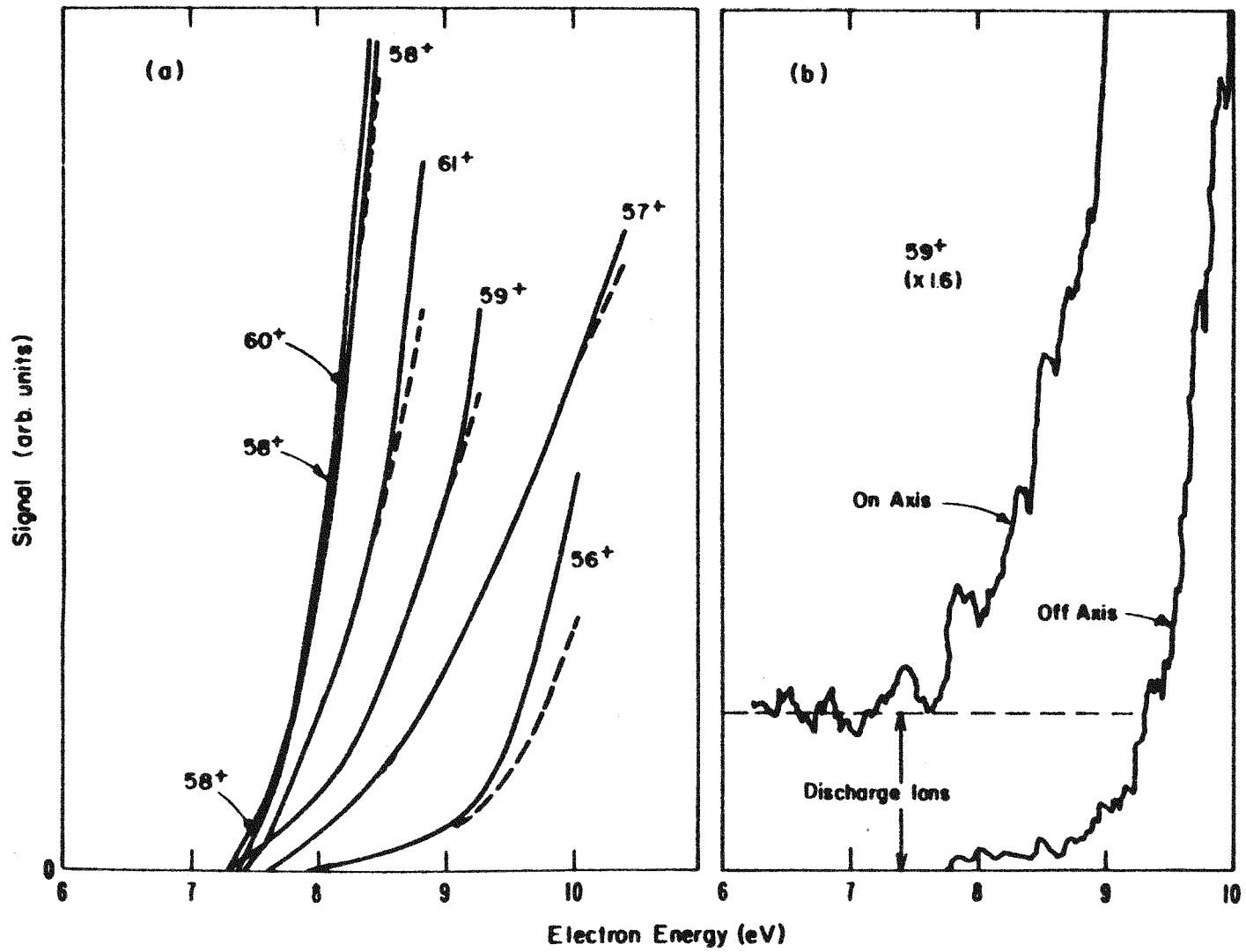

Fig. 2.4. $e + Si_2H_n \rightarrow Si_2H_n^+$ signals (left figure) from radicals produced in a 70 mTorr dc silane discharge. Except for ~10% isotopic correction, Si_2H_m occurs at mass 56 + m. An example of the method used to separate the $e + Si_2H_6 \rightarrow Si_2H_n^+$ and discharge-ion background is shown for the M = 59 case in the right figure.

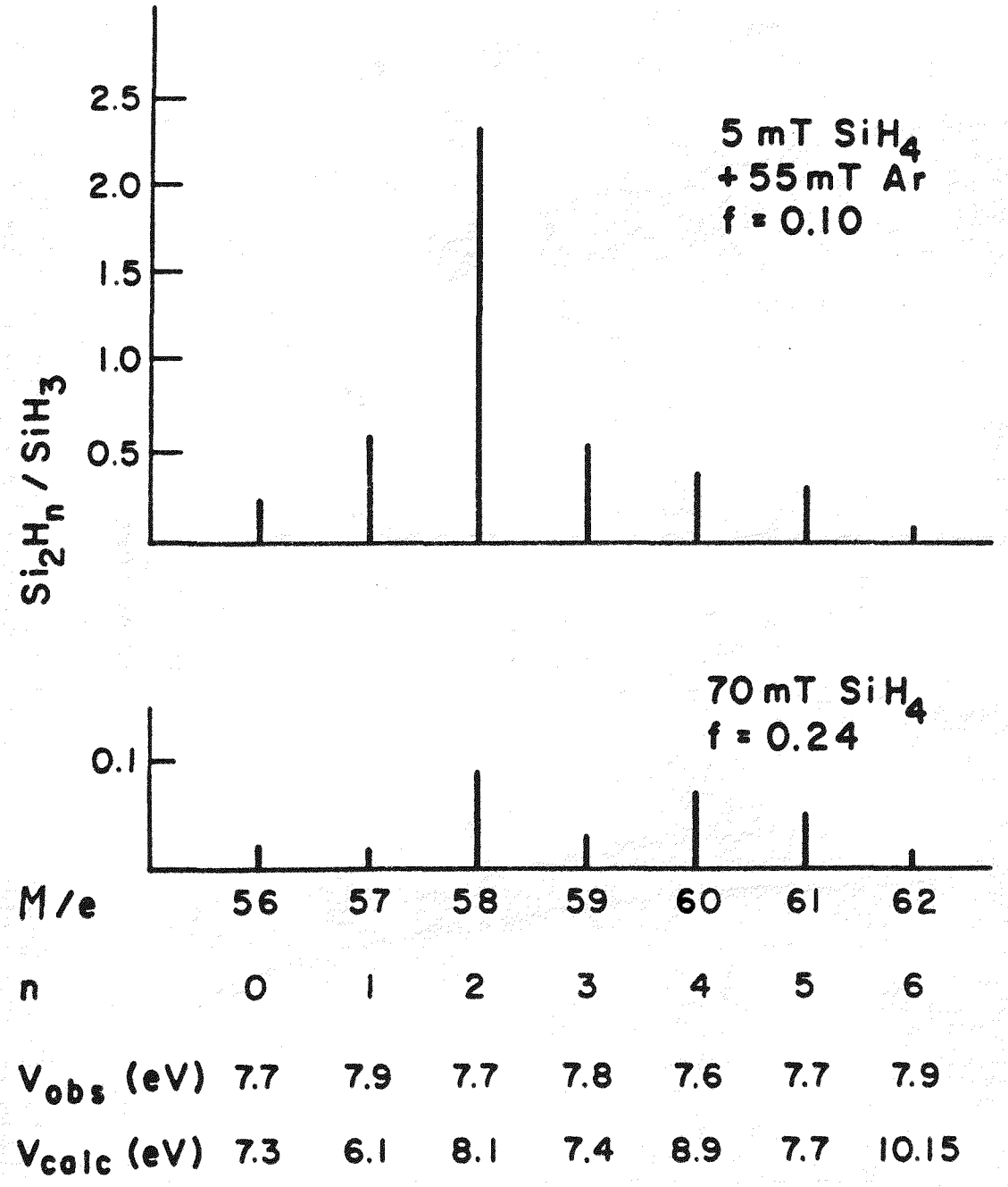

Fig. 2.5. Ratios of Si_2H_n densities relative to SiH_3, vs. mass, for dc discharges in silane and a silane/Ar mixture. The observed apparent threshold energies are shown as V_{obs}, and that calculated as V_{calc}. Both numbers are uncertain by a large fraction of 1 eV in many cases. The signal at mass 62 is attributed to heavier isotopes of Si_2H_n with n = 2-5.

SECTION 3.0

RADICAL PRODUCTION IN GAS REACTIONS

In low-pressure discharges used for production of a-Si:H films the cathode sheath fills a large part of the discharge volume, and most of the electrical energy is depositing in this sheath region. Our knowledge of electron energy distributions and collision processes in these dc discharge sheaths has been greatly improved over the last few years by detailed calculations; these are discussed by Chatham and Gallagher [9] relative to ion chemistry in silane dc discharges. Here we are interested in the neutral radical production in dc discharges, since this is the initial step in the discharge neutral chemistry that leads to film production. The discharge issues are very similar to those involved in the ion production, since the threshold for silane dissociation to neutral radicals is ~8 eV and to ions is ~12 eV. Thus, as in the ion production situation only the distribution of electron energies greater than ~10 eV in the sheath is relevant. The sheath calculations obtain a very broad distribution of energies above 10 eV, and we expect this to hold for the these silane discharges as well. Thus, most of the silane dissociation in the neutral radicals is induced by relatively high energy electrons, with energies in a broad distribution from 10-100 eV. The available data on dissociation in other molecular species, as well as qualitative models for this process, lead us to expect that the distribution of fragments is relatively independent of electron energy across this range.

Melton and Rudolph [10] have measured the dissociation of CH_4 into the CH_n radicals by 100 eV electrons. The fractionation pattern observed was that CH_3 constitutes 80% of the CH_n radicals and that atomic hydrogen exceeds the sum of all of the SiH_n radicals by about a factor of 2. We believe that this distribution is also appropriate for high-energy electrons on silane, particularly as it is dominated by the production of single hydrogen and SiH_3 radicals as we expect for high-energy electron collisions. That is, the probability of stripping one hydrogen atom from the molecule is much greater than the probability of any multiple break-up processes. This break-up pattern is shown at the right side of Fig. 3.1, corresponding to a pure silane discharge. This break-up pattern is quite different from that proposed by Perin and Schmitt [11] from comparison to the ion fractionations in silane. We believe this is due to a misinterpretation of the source of the SiH_2^+ in their interpretation of the ion fractionation pattern.

Since we had to use a SiH_4/Ar mixture to operate a self-sustained discharge at very low SiH_4 densities, we must also consider the SiH_n radical production which results from collisions with argon metastables and ions. In addition, in pure and mixed silane discharges, ion-molecule

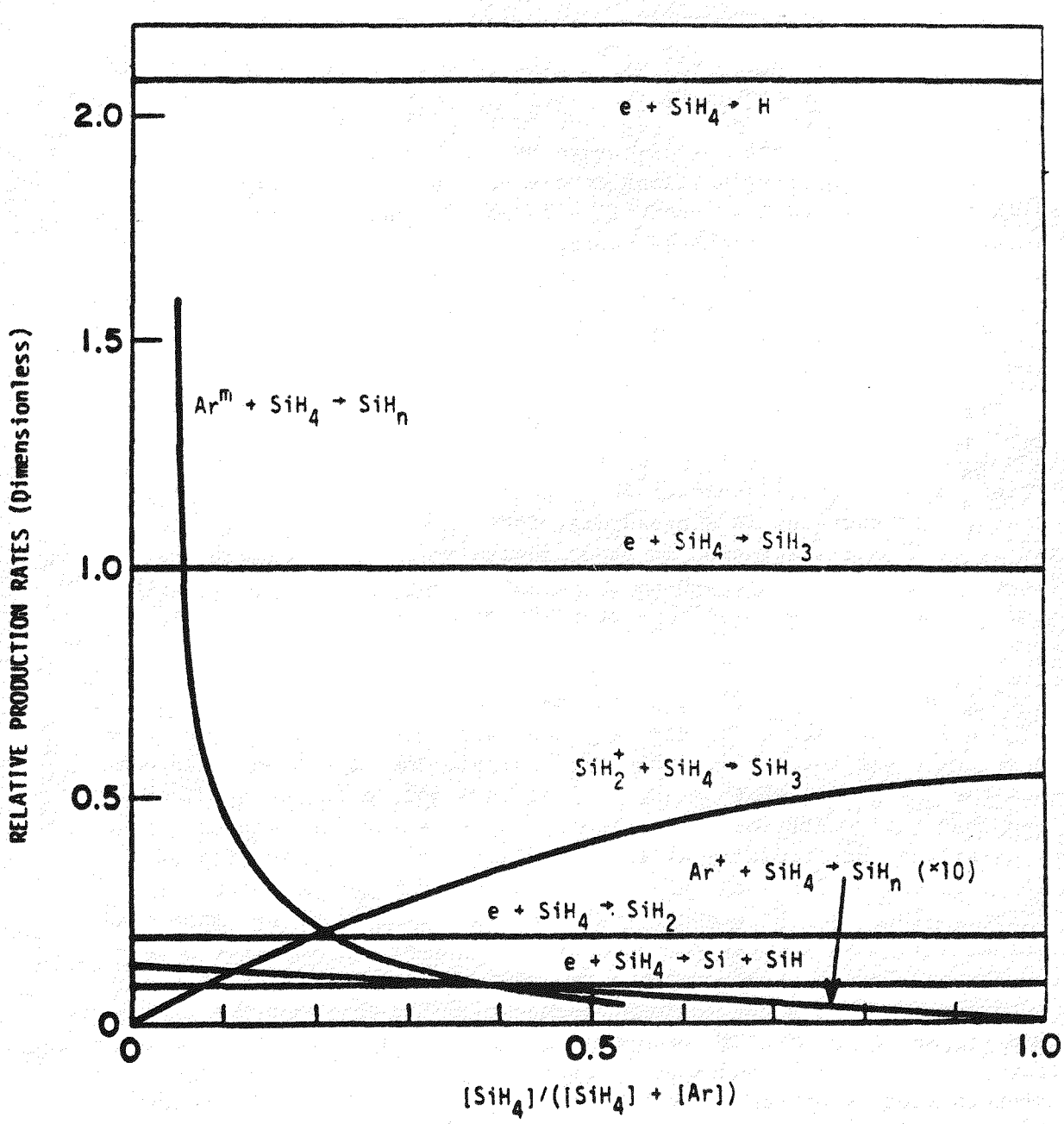

Fig. 3.1. Calculated initial rates of production of the SiH_n and H radicals in a dc discharge in an 80 mTorr silane-argon mixture, as a function of mixing fraction.

reactions as well as atomic hydrogen reactions can produce SiH_n radicals. Considering first the argon metastable reactions, we note that Balamuta et al. [8] have studied the analogous reaction of argon metastables with CH_4 and proposed that the dominant reaction channels are to CH_2, CH_3 and H. Taking the cross section for argon metastable production by high-energy electrons as that given by Chutjian and Cartwright [12] we find that this source of radicals becomes significant for silane fractions below 20% in the argon silane mixtures (Fig. 3.1). However, from the proposed break-up fractions its primary effect is to produce SiH_3 and H, which are already the dominant radicals in the discharge due to direct electron collisions. Thus, this argon metastable reaction has a relatively minor effect on the radical mixture.

Electron impact produced Ar^+ can react exothermically with SiH_4 to yield SiH_n^+ ions plus H or H_2, or endothermically to yield SiH_n radicals plus H^+ or H_2^+. The latter endothermic reactions can occur in the discharge due to the ion kinetic energy gained in the discharge sheath field. Chatham et al. have measured the $Ar^+ + SiH_4$ reaction coefficient and found it to be quite slow, i.e., 2×10^{-11} cm^3 s^{-1}. The Ar^+ ions spend ~1 μs in the discharge on the average, and this rate coefficient times the silane density and the Ar^+ dwell time yields a small reaction probability. Thus, only a few of the argon ions undergo these ion-molecule reactions before leaving the discharge. Overall, this is a minor source of neutral radicals compared to the direct electron production of such radicals (Fig. 3.1).

The ion-molecule reactions of SiH_n^+ are well known [13]. Only one of these reactions produces significant amounts of SiH_n radicals, i.e., the SiH_2^+ reaction with silane forms $SiH_3 + SiH_3^+$. (The other ion-molecule reactions produce disilane ions without forming SiH_n radicals.) Since SiH_2^+ is initially produced at nearly the same rate as SiH_3, this reaction is a major contributor of additional SiH_3 to the radical mixture. The ratios of these different sources of SiH_n radicals is summarized in Fig. 3.1.

We will now discuss the reactions of the H and SiH_n radicals in the gas phase, first considering the atomic hydrogen reactions, and then the SiH_n reactions. These are listed in Table 2.1 along with reaction enthalpies, which are estimated in some cases.

Hydrogen atoms are known to rapidly abstract an H atom from silane, with a rate coefficient of 1×10^{-11} cm^3 s^{-1}. This is process 8 of Table 2.1, which we will label R8. Similar notation, referring to Table 2.1 reactions, is used in the following discussion. As will be noted later in discussing the surface model, any H atoms that reach the surface before undergoing this abstraction reaction will abstract hydrogen atoms from the surface, leaving a dangling Si bond which will frequently abstract an H from SiH_4. Thus most of the H atoms reaching the surface

have the same effect as they do in the gas; they abstract the hydrogen from SiH_4 leading to SiH_3. As a consequence nearly all H atoms produced in the discharge are processed into SiH_3 radicals, effectively tripling the SiH_3 density. When all the sources of SiH_3 radicals are considered, SiH_3 represents more than 90% of the total SiH_n radical production (Fig. 3.1).

The reactions listed in Table 2.1 for atomic silicon are exothermic and are expected to be rapid, causing a rapid loss of Si in the gas. They are expected to have rate coefficients of about 3×10^{-12} cm^3 s^{-1} and to primarily form Si_2H_2 or two SiH_2 radicals. This adds perhaps 20% more SiH_2 to that initially produced by electron collisions. SiH_2 readily undergoes an insertion reaction with SiH_4, forming highly excited disilane that can be stabilized by a third body, but at these low pressures may frequently dissociate back to SiH_2 before stabilization. It might also stabilize by dissociating into $Si_2H_4 + H_2$, although this is not generally considered likely in the pyrolysis literature. Overall, Si and SiH_2 can react to form heavier even-hydrogen radicals, but will not form any odd-hydrogen radicals.

The significant reactions of SiH are R10 (of Table 2.1), with stabilization, and R11. Perrin and Schmidt [11] have recently reported that the SiH loss rate is fast ($k \sim 3 \times 10^{-12}$ cm^3 s^{-1}), which is to be expected since SiH can insert readily into SiH_4. Thus SiH reacts quickly to form odd-hydrogen disilane radicals.

The SiH_3 loss reactions are R13 and R14. R13 has been discussed in pyrolysis experiments [14] and is expected to be negligible under discharge conditions because of the enthalpy of reaction. R14 has been excluded from consideration in a large number of H-atom initiated decomposition and photolysis experiments [15,16]. This exclusion has not been due to the enthalpy of reaction, but is apparently because of the intuitively unreasonable transition state that the reaction implies. However, reactions R14 through R18 are included here because they might occur and because they may be important even if they are slow. In particular, R14 and R16 or R14, R15 and R18 are chain reactions which may be important in surface pyrolysis [17]. A direct experiment on these reactions would be important. In summary, there are no known fast silyl loss reactions with silane, and most of the SiH_3 produced in the discharge is expected to reach the surface.

It is important to note that in these low-pressure discharges the radicals diffuse to the surface in a typical time of a millisecond, whereas the silane is dissociated with a characteristic time of 10 s. As a result, typical radical densities are less than 10^{-4} of the neutral silane density and for these very low densities gas-phase radical-radical reactions are negligible, i.e., their probability of occurring during the millisecond diffusion time to the surface is expected to be less than

10^{-2}. Thus these deposition discharges represent a very different situation than is often considered in photolysis and other homogeneous decomposition experiments, in which radical-radical reactions are often the dominant radical loss mechanism.

The result of these considerations is summarized in Fig. 3.2, where the calculated Si, SiH, and SiH_2 densities (dashed lines) are compared to the measured densities (solid lines). These calculated densities come from consideration of only gas production and gas reactions. Thus, the much larger measured, vs. calculated, Si and SiH densities in Fig. 3.2 indicate that the principal source of Si and SiH is release from the surface. This is almost certainly due to sputtering, as these radicals cannot be produced by surface reactions due to their high enthalpies. This interpretation is also consistent with the increase in these radical densities, relative to SiH_4, at the left side of Fig. 3.2, i.e. surface sputtering will become more important relative to gas dissociation of SiH_4 as the SiH_4 density decreases. The measured SiH_2 density is also significantly larger than the calculated density, but this difference is within the uncertainty in our calibration procedures and calculation. We have not indicated the measured and calculated SiH_3 densities in Fig. 3.2, as they are much larger. The above considerations lead to a calculated $SiH_3/\Delta SiH_4 \cong 3 \times 10^{-4}$, while the measurements yielded about 1.5×10^{-4} for all silane/argon ratios. As with SiH_2, this factor of 2 difference between measured and calculated densities is within the uncertainties in the measurements and the assumptions used to reduce the raw data to densities. Thus, we conclude that most (or all) of the observed SiH_3 and SiH_2 is due to gas production and gas processes.

From these results, it is apparent that film growth is almost entirely due to SiH_3 incorporation into the surface, particularly in the pure silane discharges normally used for production of photovoltaics. The manner in which this incorporation can occur will be discussed in the next section. A relatively small percentage of the film growth is also due to incorporation of SiH_2, SiH, Si, and heavier radicals Si_2H_n, etc., and sputting of the film surface plays a major role in producing these Si, SiH and heavier radicals. Since the photovoltaic quality of the bulk film depends on very low trap densities, incorporation of these minor radical constituents could play a major role in determining film quality.

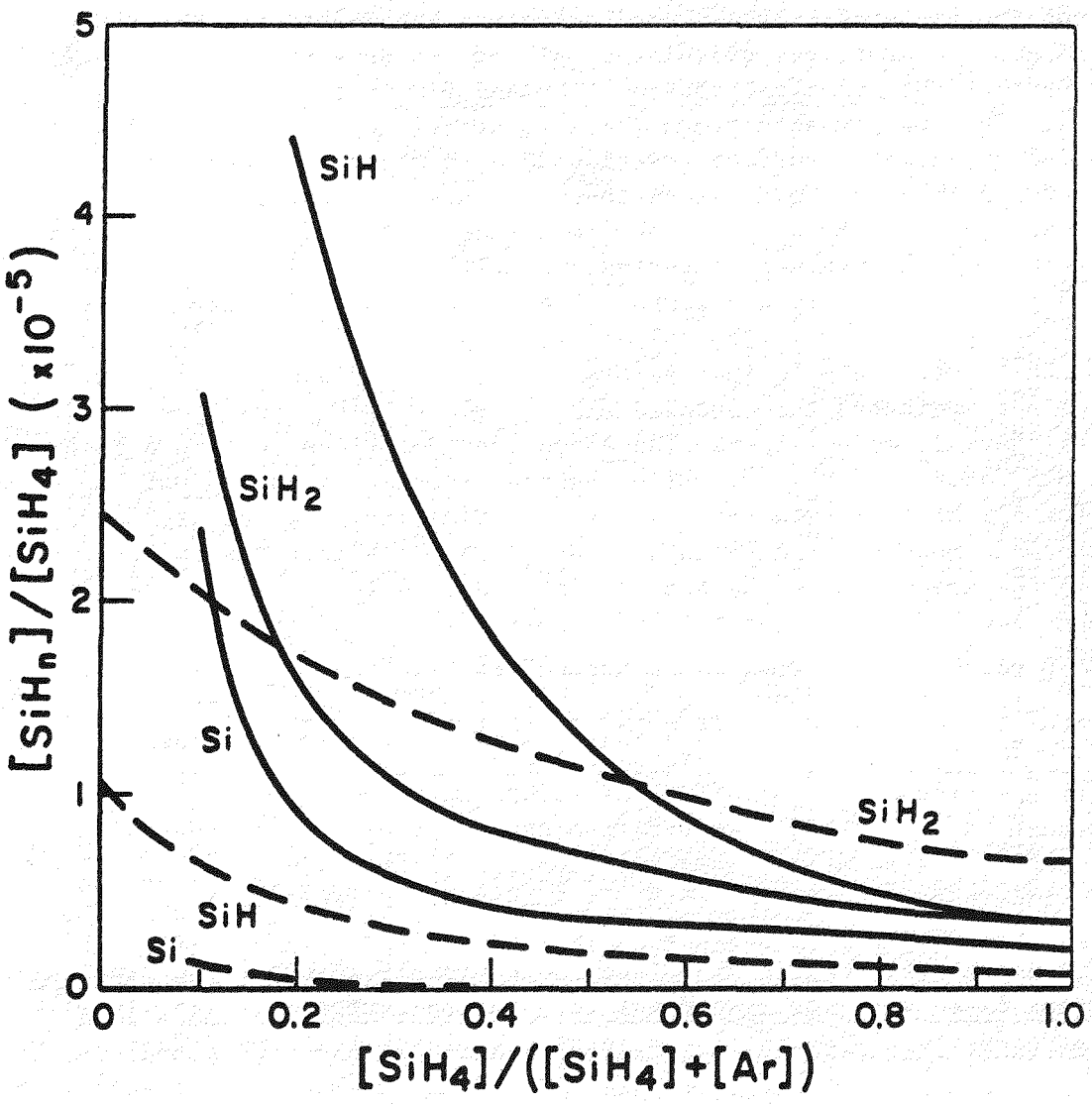

Fig. 3.2. Calculated relative radical densities, $[SiH_n]/[SiH_4]$ for n = 0-2, shown vs. fraction of silane in the silane-argon mixture (dashed lines). Smoothed data from dc discharges in ~80 mT total pressure, with silane depletion f ≅ 0.1, are represented by the solid lines.

SECTION 4.0

SURFACE REACTION MODEL

There is little direct evidence regarding the reactions of radicals and neutral silane species with a growing a-Si:H surface. Measurements of reactions on crystal silicon are only slightly relevant, due to the completely different structure of the growing amorphous surface. The radicals and ions initially incorporated into the a-Si:H surface have a H/Si ratio of 2 to 3, while the ratio in bulk a-Si:H films is known to be 0.03 to 0.3 for substrate temperatures of 300 to 0°C. We expect this transition from a hydrogen-rich surface to a hydrogen-poor film to occur in several atomic layers, with gradually increasing Si-Si bonds accompanied by H_2 elimination with increasing depth.

To discuss gas-surface reactions, a model of the wall will now be proposed in which the surface and first several monolayers below the surface are considered. Each surface silicon atom has at least one Si-Si bond connecting it to the film and the remaining one, two, or three bonds are assumed to be saturated with H atoms. (A very small fraction of the silicon surface atoms will have an unsaturated bond, as will be discussed below.) This top monolayer will have an H-content of several hundred atomic percent (relative to silicon), while successively deeper layers will have lower H-content until the bulk material value of 3-30% of silicon is reached. The gradient in H-content will depend on the rate of removal of the H atoms through several possible reactions.

One reaction that eliminates H from the film involves the breaking of two neighboring Si-H bonds below the surface and the formation of an H-H bond and a Si-Si bond. This reaction is exothermic, although it does require a four-atom transition state. The rate of this reaction is unknown. The analogous gas reaction, $2\ SiH_4 \rightarrow Si_2H_6 + H_2$ is slow, but in the solid-state the species are confined and this reaction can easily be faster than the deposition rate of typically one monolayer per second.

Another possible reaction that removes hydrogen from the film involves the catalytic behavior of free H atoms or dangling bonds within the solid [18]. (The presence of free H atoms or dangling bonds in the solid will be discussed below.) A free H atom can abstract a bound H atom, forming H_2 and a dangling bond. The dangling bond then reacts with an Si-H bond forming an Si-Si bond and a free H atom. The equivalent gas-phase reaction (R13) is endothermic by ~16 kcal/mole, which suggests that this could be an important cause of H_2 evolution. However, H_2 evolution from post-discharge heated films have been observed to have smaller activation energies [19].

The well-known H-content dependence on wall temperature [4] is presumably determined by the enthalpies of this hydrogen removal process. If the H_2 removal process is slow relative to the growth rate (typically one monolayer per second), the top several monolayers are expected to have a polymeric type structure, $(SiH_2)_n$. A faster removal rate or slower growth rate should allow more Si-Si bonding from shorter chains, presumably resulting in different film structure.

Under the conditions of discharge deposition we expect almost all of the dangling silicon bonds on the surface to be attached to hydrogen atoms. Such a region of the surface is shown diagrammatically at the upper left of Fig. 4.1. Here the gas-phase Si atoms are indicated as large, open circles and the H atoms as small solid circles. The surface Si atoms connected to the film are indicated as semicircles protruding above a line. Each of these surface Si atoms is assumed to have three filled bonds that are not shown, of which one or more is to other Si atoms in the film. A line corresponding to the fourth bond is drawn upward, toward the gas. We label these upward bonds as b or $\bar{b}$ when empty or occupied by an H atom.

When stable neutral silanes collide with this H-coated surface, they bounce off or are adsorbed very weakly. When an Si, SiH, or SiH_2 radical collides with this surface, it can incorporate immediately with a Si-H bond, as indicated in the top row of Fig. 4.1 for the SiH_2 case. (We use $(SiH_3)_s$ to indicate an SiH_3 incorporated permanently onto the surface with a Si-Si bond.) When an SiH_3 arrives at the surface, as indicated at the left of the second row of Fig. 4.1, it forms a weakly bonded surface state, labeled A, that is shown in the third row. As indicated in the figure, this intermediate state A can return an SiH_3 or SiH_4 to the gas, or incorporate as $(SiH_3)_s$ with the release of H or H_2. All of these states contain one dangling bond, hence have nearly the same enthalpy, i.e., b, A, and SiH_3 each contain one dangling Si bond. Several SiH_3 and SiH_4 releases may occur before incorporation. This would lead to a low effective sticking coefficient for SiH_3, and homogeneous surface coverage, as observed Knights [20] under low-power conditions. However, the SiH_3 density we observe corresponds to few such desorptions, and Knight's observations could instead be explained by rapid surface hopping of dangling bonds.

A second channel for incorporation of SiH_3 into the surface is by the interaction of two radicals on the surface, i.e., if A + b, A + A, b + SiH_3, or A + SiH_3 can arrive at the same or adjacent sites, then these can recombine. These two-radical processes are indicated diagrammatically on the right side of Fig. 4.1. These incorporation reactions release the energy of two bonds (~180 kcal/mole), as in the gas reaction $2SiH_3 \rightarrow Si_2H_6$. Thus, Si_2H_6 released during incorporation may be highly excited, and could dissociate into $Si_2H_4 + H_2$ or even $Si_2H_2 + 2H_2$. This

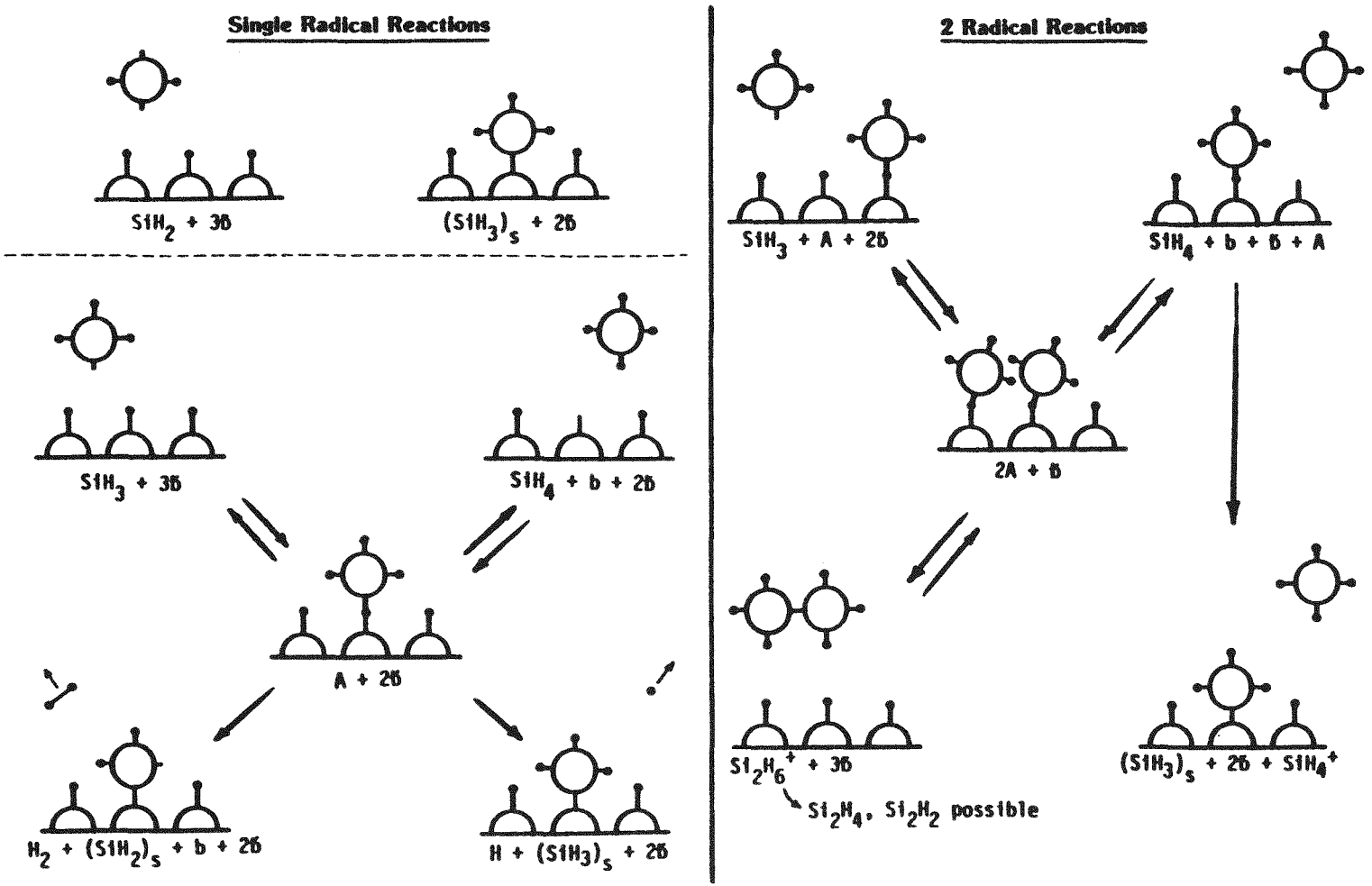

Fig. 4.1. Idealized diagram of the radical-surface reactions leading to Si incorporation (film growth) and gas release.

Si_2H_2 and Si_2H_4, although more stable than the odd-H radicals due to the even number of bond pairs, should incorporate fairly readily into the surface. Certainly once a surface dangling bond is freed by hydrogen abstraction, this should happen rapidly. Thus this source of Si_2H_2 and Si_2H_4 (at most one from each pair of SiH_3 consumed) is also insufficient to explain the observed densities. Energetic ion surface bombardment thus appears still more likely as the primary cause of radical release.

An H atom, formed in the discharge or released from the surface can also abstract an H atom from the surface, forming an H_2 molecule and an open site ($H + \bar{b} \rightarrow H_2 + b$). Thus, H atoms reacting with the surface induce film growth equivalent to SiH_3. The SiH_3 and SiH_4 in the second row, left side of Fig. 4.1, can be replaced by Si_2H_5 and Si_2H_6, respectively. Thus any Si_2H_5 formed by $SiH_3 + SiH_4$ reaction can be converted to Si_2H_6 at the surface while assisting film growth ($Si_2H_5 + \bar{b} \rightarrow Si_2H_6 + b$). This and the process $2SiH_3 + 2\bar{b} \rightarrow 2A \rightarrow Si_2H_6 + 2\bar{b}$ diagrammed in Fig. 4.1 could convert a large fraction of the SiH_3 into Si_2H_6, and this appears a very probable source of much of the observed Si_2H_6.

Following the incorporation of these heavily hydrogenated forms of Si_xH_m, with the average m/x in excess of 2, H_2 must be released by simultaneously breaking two Si-H bonds to form an H-H and a Si-Si bond, until the surface ultimately reaches the m/x = 0.03-0.3 ratio of the amorphous silicon film. This Si-Si bonding can also be initiated when a radical abstracts a hydrogen from the surface, since the resulting dangling bonds can migrate below the surface as well as along it. Note also that some incorporation, such as the $SiH_4 + b + 2\bar{b} \rightarrow A + 2\bar{b} \rightarrow H_2 + (SiH_3)_s + b + 2\bar{b}$ steps on the left side of Fig. 4.1, preserve dangling bonds and can act as chain reactions.

This very preliminary picture given for the surface reactions does not yet propose different roles that the different radicals might play in determining film quality. We are currently at the stage where we have identified what we believe to be the dominant species and processes responsible for deposition and film growth, but we have no quantitative data or models for the important mechanisms leading to the film characteristics. Perhaps the greatest progress is in the types of measurements which we are now capable of doing and have achieved. If we can now measure detailed dependences of the radical mixtures on parameters such as pressure, pumping speed, discharge current, discharge type and shape, surface temperature, time and other factors, this should allow a better separation and understanding of the gas and surface processes.

SECTION 5.0

CHEMICAL VAPOR DEPOSITION MEASUREMENTS

The surface reactions occurring in glow discharges (GD) may be closely related to those occurring in chemical vapor deposition (CVD), and comparisons of GD and CVD data may illucidate our surface model. For example, we have observed SiH_4 released from heated surfaces exposed to Si_2H_6, and (in lesser amounts) Si_2H_6 from surfaces exposed to SiH_4. Farrow [21] has also observed Si_2H_6 from SiH_4 decomposition on silicon. The surface processes we must invoke to explain this are very similar to those needed to explain the discharge data. Thus, we plan to continue measurements of decomposition on hot surfaces to improve our understanding of these surface reactions.

In Fig. 5.1 the rate k_1 of SiH_4 decomposition we measured [22] at 710 K is compared to the pyrolysis measurements of Purnell and Walsh [23] (line) and of Ring and O'Neal [17] (point), at the same temperature. Our data are due to surface decomposition, whereas Purnell and Walsh and Ring and O'Neal attribute their observed decomposition to homogeneous decomposition. Both of these are plotted in Fig. 5.1 as an effective rate $k_1 = d\ell n[SiH_4]/dt$ by assuming a typical volume/surface ratio. The expected pressure dependence of the homogeneous decomposition calculated by Ring and O'Neal [17], is shown as a dashed line. We have also included in Fig. 5.1 measurements of silane decomposition on a crystal Si surface by Gelain et al. [24] and by Farrow [21] at ~1200 K, and a shock-tube pyrolysis measurement by Ring and O'Neal (attributed to homogeneous decomposition) at a similar temperature [17]. As can be seen, the heterogeneous (surface) decomposition dominates at pressures below 10 Torr at either temperature, for this typical Volume/Surface ratio. This fact is accepted by researchers in this field [17,25], but the decomposition initiation mechanism above 10 Torr is still in dispute; whether the homogeneous mechanism or a heterogeneous mechanism is dominant [17,22,25].

We have now analyzed a large array of silane CVD data from our laboratory, for surface temperatures of 700-2000 K, silane pressures of 10^{-3} to 10^{2} Torr, and various silane-H_2 mixtures. (Some of these data and preliminary conlusions were published in Ref. [22]). Most results of these extensive measurements, taken with four different apparatus configurations and including detailed product-specie measurements, can be explained by a relatively simple model for the gas-surface interactions. These measurements and their interpretation are discussed in detail in R. Robertson's thesis, which was submitted to the University of Colorado on May 30, 1985 (unpublished). Here we will give a very brief summary of this model, since it will be described in detail in future publications.

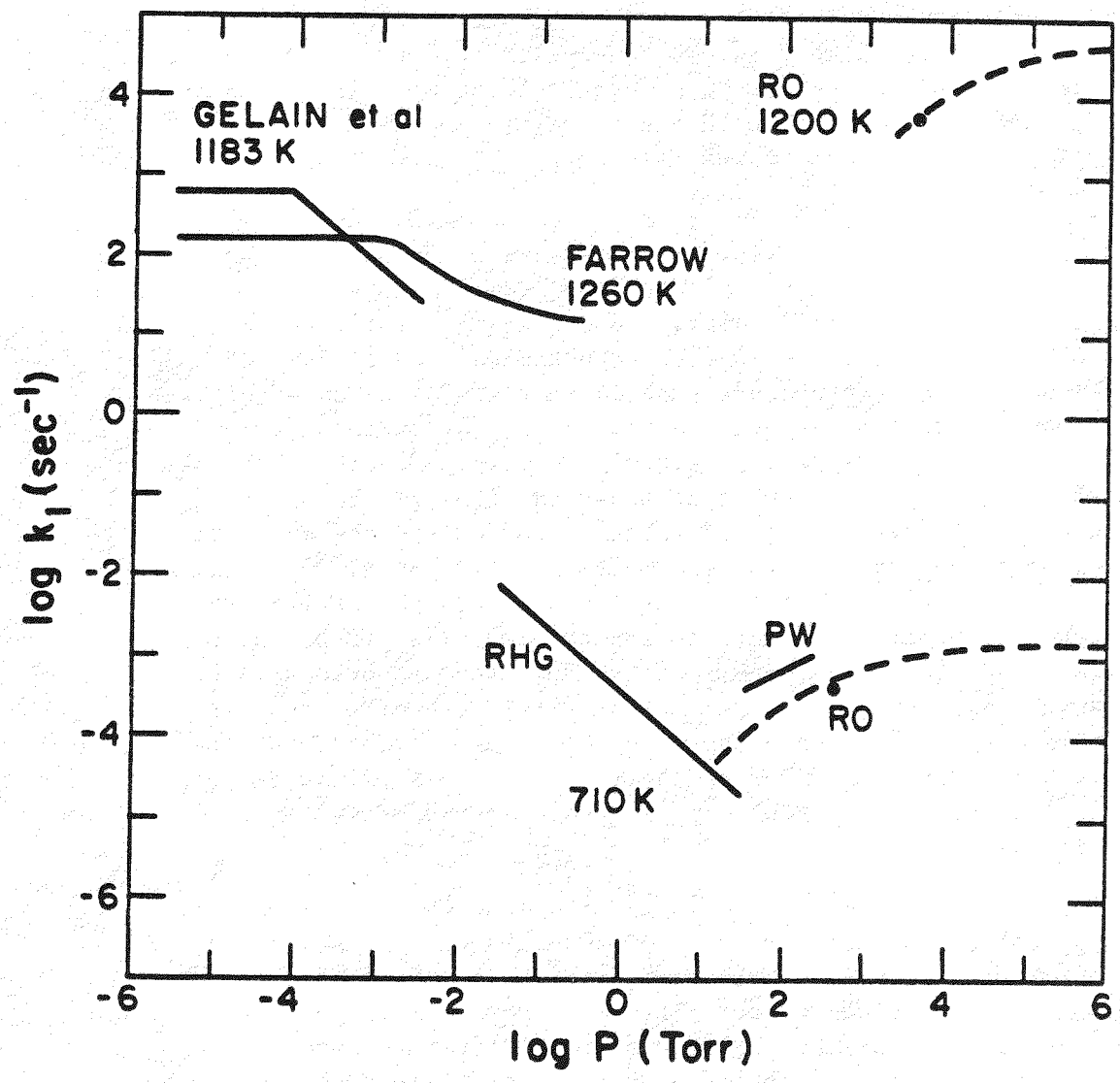

Fig. 5.1. Silane pyrolysis rate measurements, vs. silane pressure. The heterogeneous decompositions (solid lines labeled Gelain, Farrow and RHG) are placed on the same scale as the homogeneous rates (RO and PW lines) using a volume/surface ratio equivalent to a 6 cm diameter cylinder.

As described in the previous section and shown diagrammatically in Fig. 4.1, almost all surface Si atoms have their surface bonds filled with H atoms. If the typical Si-H bond energy is 80 kcal/mole, or slightly less than the gas value, then H atoms are very infrequently released at pyrolysis temperatures below 1500 K. However, a pair of surface H atoms will occasionally vibrate into close proximity, allowing the formation of H_2, which is released into the gas. This leaves two dangling Si bonds, which require 2 × (~80 kcal/mole), while the H_2 bond (104 kcal/mole) is regained. Thus the net enthalpy change for H_2 release is (2 × 80-104 = 56) kcal/mole. As these dangling Si surface bonds migrate separately about the surface, an SiH_4 from the gas occasionally collides with one and is adsorbed. If a second dangling bond migrates to this adsorbed SiH_4 before desorption, the SiH_4 can be incorporated into the surface, as SiH_3, while the two dangling bonds are refilled with H atoms. This is an exothermic reaction, but requires dangling Si bonds at adjacent sites. At high pressure and low temperature, the rate-limiting step in this CVD of silane is the H_2 elimination necessary to free dangling Si surface bonds. Thus, a 56 kcal/mole activation energy and pressure-independent rate is observed for CVD at temperatures below 900 K and pressures above 1 mTorr. At higher temperatures and low pressure, the H_2 elimination is faster than SiH_4 arrival at the surface, and a CVD rate proportional to pressure with a lower activation energy is observed.

If there is H_2 as well as SiH_4 in the gas, each surface Si dangling bond may adsorb H_2 as well as SiH_4. If a second dangling bond migrates to an adsorbed H_2, then it may incorporate back into the surface as two Si-H bonds, releasing 56 kcal/mole into the solid. This reverse of the H_2-release step competes with SiH_4 incorporation as a sink for dangling Si surface bonds, so H_2 gas inhibits the CVD process. This inhibiting only occurs at the lower temperatures and higher pressures, where H_2 elimination is the CVD rate-limiting step. Thus, we observed it in our lower T data, but we and other researchers failed to observe it at higher temperatures. This simple model can now quantitatively explain essentially all of our CVD data, as well as that of earlier researchers, and it logically resolves several apparent contradictions between reported pressure, temperature, and H_2 dependences. We believe this is an essential, major step toward developing a detailed understanding of a-Si:H film growth, in discharges as well as in CVD reactors.

SECTION 6.0

RAMAN SPECTRA

Under the direction of J. Scott, the Raman spectra of several types of a-Si:H films produced at SERI have been measured. Raman shifts of 50-1100 cm^{-1} were obtained from 0.1-0.5 μm thick films. A spectrum from an a-Si:Sn,H film is compared to that of an intrinsic a-Si:H film in Fig. 6.1. This comparison shows that the a-Si:Sn,H film contains many more SiH_x sites (seen [26] at 600-700 cm^{-1}) and Si_3-SiH sites (seen [27] at 210 cm^{-1}) than the a-SiH film.

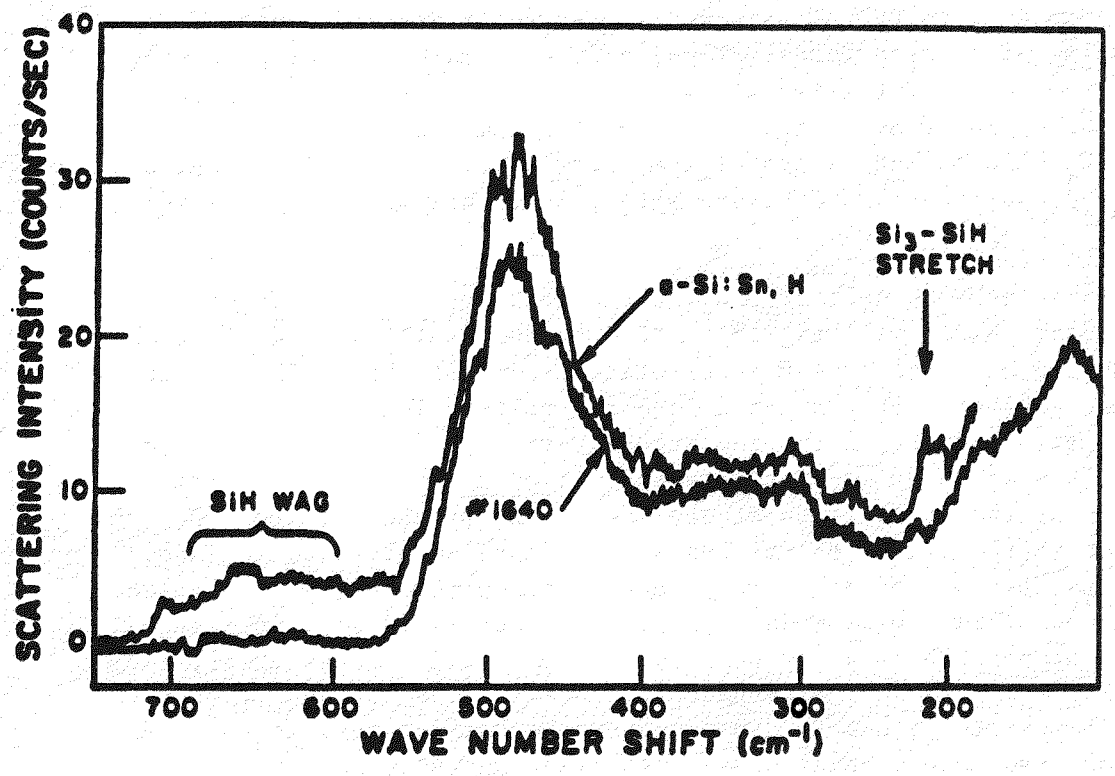

Fig. 6.1. Raman spectrum of an intrinsic, T_s = 230 C, a-Si:H film (#1640), and a silicon-tin alloy film.

SECTION 7.0

CONCLUSIONS

We have been able to increase the radical-detection sensitivity of our apparatus, allowing radical densities as low as $10^8/cm^3$ to be measured. We have also devised a method to separate Si_2H_n radical signals from Si_2H_6 produced in the discharge, and we can now detect radical/SiH_4 ratios as low as 10^{-6}. Using these improved sensitivities we have measured the SiH_n and Si_2H_n radicals from dc discharges, for pure silane and silane-argon mixtures. From these data and our models, we have concluded that the SiH_3 radical is formed in the gas and is primarily reponsible for film growth. One consequence of this, rather than SiH_2, SiH and Si deposition, is a propensity for a smoother, more uniformly structured film due to surface diffusion of SiH_3 before incorporation by pair-reactions. Most of the other radicals seen in the gas, particularly Si, SiH, and $Si_2H_n(n=0-4)$, are not a result of gas-phase collisions, but are released from the surface due to a combination of chemical reactions and ion sputtering. The Si_2H_2 and Si_2H_4 radicals in particular are present at a large fraction of the SiH_3 concentration in a pure silane discharge. Since even a small concentration of deleterious sites in the bulk film can critically affect solar-cell efficiency, deposition of these other radicals are potentially very important, as are surface sputtering processes, in determining film quality. In a dc proximity or an rf screened-substrate discharges, these radicals sputtered from the screen can react in the gas to form long chains, which then deposit on the substrate. Also, mild sputtering of the substrate may be advantageous through the removal of long chains, or the breaking of highly-distorted Si-Si bonds to allow repositioning before they are overlaid and frozen into the bulk material.

We have developed a surface-reaction model that explains the basic steps involved in a-Si:H film growth in glow discharges and in CVD. This model, which includes an H_2 inhibiting reaction with the surface, explains a wide range of CVD data on a-Si:H from our laboratory as well as studies on crystalline silicon from other laboratories. This model can also explain glow-discharge deposition, and the resulting Si_2H_6 release from the surface which we and Longeway and Wiekliem have observed. Many details of this model, such as surface diffusion rates, need to be filled in, and we are devising and carrying out experiments for this purpose. When more details are understood, we should have a basis for understanding of the causes of SiH_3, SiH_2, SiH, and dangling-bond structures in the film.

We have completed and published a calculation of the ion production, reaction chemistry, and species reaching the surfaces of dc silane discharges. We do not yet know the effect these various ions have on the

structure and photovoltaic quality of the a-Si:H film, but this calculation provides a basis for understanding and varying this ion mixture in a systematic fashion, and for using ion measurements as a tool for discharge diagnostics.

REFERENCES

[1] R. Robertson, D. Hils, H. Chatham and A. Gallagher, Appl. Phys. Lett. 43, 544 (1983).

[2] See Abstracts of Presentations, Amorphous Silicon Subcontractors Annual Review Meeting, 21-23 March 1985 (Solar Energy Research Institute, Golden, CO), p. 67.

[3] D. E. Carlson, R. S. Crandall, B. Goldstein, J. J. Hanak, A. R. Moore, J. I. Pankove, and D. L. Staebler, Final Report, DOE Contract EY-76-C-03-1286 (October 1978).

[4] D. E. Carlson, in Polycrystalline and Amorphous Thin Films and Devices, L. L. Kazmerski, Ed. (Academic, New York, 1980), p. 175.

[5] P. A. Longeway, H. A. Weakliem and D. R. Estes, J. Phys. Chem. 88, 3282 (1984).

[6] A. Gallagher and J. Scott, Final Report, DOE Contract XB-2-02189-1 (April 14, 1982).

[7] H. Chatham, D. Hils, R. Robertson and A. Gallagher, J. Chem. Phys. 79, 1301 (1984).

[8] J. Balamuta, M. F. Golde and Y.-S. Ho, J. Chem. Phys. 79, 2822 (1983).

[9] H. Chatham and A. Gallagher, J. Appl. Phys. (in press).

[10] C. E. Melton and P. S. Rudolf, J. Chem. Phys. 47, 1771 (1967).

[11] J. Perrin and J. P. M. Schmitt, Chem. Phys. 67, 167 (1982).

[12] A. Chutjian and D. C. Cartwright, Phys. Rev. A 23, 2178 (1981).

[13] G. Hess and F. Lampe, J. Chem. Phys. 44, 2257 (1968).

[14] J. H. Purnell and R. Walsh, Proc. Roy. Soc. Ser. A 293, 543 (1966).

[15] G. Orbrich, P. Potzinger, B. Reimann and R. Walsh, Organomet. 3, 1267 (1984).

[16] N. L. Arthur and T. N. Bell, Rev. Chem. Intermed. 2, 37 (1978).

[17] (a) H. E. O'Neal and M. A. Ring, Chem. Phys. Lett. 107, 442 (1984). (b) M. A. Ring and H. E. O'Neal, "Proc. Flat Plate Solar Array Workshop on the Science of Silicon Materials Preparation," (DOE/JPL-1012-81) JPL Publ. 83-13, 63 (1983).

[18] I. Haller, private communication to Alan Gallagher.

[19] F. J. Kampas and R. W. Griffith, Appl. Phys. Lett. 39, 407 (1981); J. A. McMillen and E. M. Peterson, J. Appl. Phys. 50, 5238 (1979); F. J. Kampas, J. Appl. Phys. 53, 6408 (1982).

[20] J. Knights, Proceedings of Materials Research Society Fall Meeting, Nov. 26-30, 1984, Boston, Massachusetts (1984).

[21] R. F. C. Farrow, J. Electrochem. Soc. 121, 899 (1974).

[22] R. Robertson, D. Hils and A. Gallagher, Chem. Phys. Lett. 103, 397 (1984).

[23] J. H. Purnell and R. Walsh, Proc. Roy. Soc. A 293, 543 (1966).

[24] C. Gelain, A. Cassuto and P. LeGoff, Bull. Soc. Francaise de Geramique 80, A431 (1968).

[25] J. H. Purnell and R. Walsh, Chem. Phys. Lett. 110, 330 (1984).

[26] M. Cardona, Phys. Stat. Sol. B118, 463 (1983).

[27] C. C. Tsai and R. J. Nemanich, J. Non-Crystal. Sol. 35, 1203 (1980).